Bifurcation of self-motion depending on the reaction order

Bifurcation of self-motion depending on the reaction order

Masaharu Nagayama [a, b], Masaaki Yadome [c], Mai Murakami [d], Noriko Kato [e], Junko Kirisaka [e], and Satoshi Nakata [d,e,*]

a. College of Science and Engineering, Kanazawa University, Kakuma-machi, Kanazawa 920-1192, Japan

b. PRESTO, Japan Science and Technology Agency, 4-1-8, Honcho Kawaguchi, Saitama, 332-0012, Japan

c. Graduate School of Natural Science and Technology, Kanazawa University, Kakuma-machi, Kanazawa 920-1192, Japan

d. Graduate School of Science, Hiroshima University, Kagamiyama 1-3-1, Higashi-Hiroshima 739-8526, Japan

e. Department of Chemistry, Nara University of Education, Takabatake-cho, Nara 630-8528, Japan

Key words: self-motion, bifurcation, reaction order, air/water interface; interfacial tension

*Corresponding author. Tel: +81-82-424-7409; Fax: +81-82-424-7409;

E-mail: nakatas@hiroshima-u.ac.jp

Abstract

As a simple example of an autonomous motor, the characteristic features of self-motion coupled with the acid-base reaction were numerically and experimentally investigated at the air/aqueous interface. Oscillatory and uniform motion were categorized as a function of the reaction order by numerical computations using a mathematical model that incorporates both the distribution of the surface active layer developed from a material particle as the driving force and the kinetics of the acid-base reaction. The nature of the self-motion was experimentally observed for a boat adhered to a camphor derivative with a mono- or di-carboxylic acid on a phosphate aqueous phase as the base.

1. **Introduction**

Studies of artificial motors that mimic biological motors are important not only for understanding chemo-mechanical transduction in biological systems but also for creating novel artificial motors which adapt to the environment.[1] All motor organs or organelles in living organisms work under almost isothermal and nonequilibrium conditions, e.g., a flagellar motor is driven by the membrane potential of potassium ion and pH gradient. Several artificial systems that exhibit self-motion under conditions of chemical nonequilibrium have been studied experimentally[2-15] and theoretically[16-19] under almost isothermal conditions.

More than a century ago, the self-motion of small camphor scrapings floating on water was explained by Van der Mensbrugghe as being due to the diminished surface tension of water. Subsequently, Rayleigh studied the retarding effect of contaminating oily substances on the self-motion of a camphor scraping.[20]

Recently, we reported that the nature of the self-motion of a camphor scraping changes depending on both the internal conditions (e.g., scraping morphology and chemical structure of the camphor derivative)[21-24] and external conditions (e.g., temperature, surface tension, and the shape of the cell),[24-28] and the essential features of self-motion could be reproduced by a computer simulation.[21-28] In one of these studies, we reported that the mode of self-motion of a camphoric acid boat characteristically changes depending on the concentration of phosphate ion or pH in the aqueous phase, and that the characteristic mode-change between uniform, oscillatory, and no motion is coupled with the acid - base reaction.[22]

In this study, we investigated the nature of self-motion depending on the reaction order of the acid-base reaction. A bifurcation diagram of motion (oscillatory and uniform motion) as a function of the reaction order of two chemical substances was obtained by

numerical calculation coupled with the Newtonian motion equation and reaction-diffusion equation. The features of bifurcation were also observed for a camphor derivative with a mono-carboxylic acid or di-carboxylic acid in actual experiments.

2. Experimental section

Camphanic acid and other chemicals were obtained from Sigma-Aldrich (St. Louis, MO). Water was first distilled and then purified with a Millipore Milli-Q filtering system (pH of the obtained water: 6.3, resistance of water: > 18 MΩ).

Camphoric acid or camphanic acid was packed into a pellet die set (3 mm diameter, 1 mm thickness). A camphoric acid or camphanic acid disk, which was connected to the back of a polyester plastic boat (thickness: 0.1 mm, 4 x 6 mm, 2 mg), was floated on an aqueous phase (2 ml) in a linear chamber (length: 300 mm, width: 5 mm, depth: 2 mm) composed of Teflon to simplify the analysis of the motion by control of its direction. At this stage, the boat moved in the direction of the side of the boat without the disk. To obtain high reproducibility for this phenomenon, the same camphoric acid or camphanic acid boat (mass: 3 mg) was prepared, i.e., the size and shape of the camphor derivatives and how the disk was attached to the boat were almost the same in each experiment.

The movement of the camphoric acid scraping was monitored with a digital video camera (SONY DCR-HC48) and recorded on videotape at 293 ± 1 K. The minimum time resolution was 1/30 sec. The movement of the boat was analyzed by image-processing and -analysis software (Image J, National Institutes of Health, USA).

3. Results

Figure 1 shows (a) a phase diagram of the motion of camphanic acid and camphoric acid boats depending on the concentration of Na_2HPO_4 in the aqueous phase and (b) the time

variation of the velocity of the boats with different concentrations of Na_2HPO_4 (0.02 and 0.08 M). The camphanic acid boat showed only uniform motion at the concentrations of Na_2HPO_4 examined. In contrast, the camphoric acid boat showed uniform motion at the lower concentration (Fig. 1b-3), but the uniform motion changed to intermittent oscillatory motion, i.e., repetition among rapid acceleration, slow deceleration, and rest, when the concentration was greater than 0.05 M (see Fig. 1b-4). In the Figure, the thickness of the gray line corresponds to the concentration region within which it is difficult to distinguish between uniform and intermittent oscillatory motion.

In Fig. 1b, the movement of the boat was analyzed around the center of the chamber, excluding 50 mm from both ends to eliminate the influence of the boundary of the chamber. In Figs. 1b-1, 1b-2, and 1b-3, the boat rapidly reached uniform motion within 0.3 s after it was placed on the aqueous phase, i.e., these graphs were plotted immediately after the boat reached uniform motion. The pH in Fig. 1b at the initial stage was 9.0. After the boat had moved, the pH around the center of the chamber changed to 8.6-8.8.

Figure 2 shows (a) the velocity of uniform motion and (b) the period of the intermittent motion of a camphoric acid boat depending on the concentration of Na_2HPO_4 in the aqueous phase. The velocity and period are averaged value from four examinations. The velocity of motion decreased with an increase in the concentration of Na_2HPO_4 within the concentration region of uniform motion. The period of motion increased with an increase in the concentration for intermittent oscillatory motion. The velocity of uniform motion for the camphanic acid boat monotonically decreased with an increase in the concentration of Na_2HPO_4, and was higher than that for the camphoric acid boat (data not shown).

4. Discussion

4.1. Mechanism of the characteristic motion coupled with the chemical reaction

Based on the experimental results and a related paper[22], we can consider why the camphanic and camphoric acid boats showed motion with different features depending on the concentration of Na_2HPO_4. The following acid-base reaction is generated in this experimental system:

$$\text{R-(COOH)}_n + n\text{HPO}_4^{2-} \xrightarrow{k_r} \text{R-(COO}^-)_n + n\text{H}_2\text{PO}_4^- \quad (1)$$

where R-(COOH)_n are organic acids (R: organic body, *n*: number of carboxyl groups), and HPO_4^{2-} acts as a base. In our experiment, R = C_8H_{14} and *n*=2 for camphoric acid, and R = $C_9H_{11}O_2$ and *n*=1 for camphanic acid. We previously reported that surface active R-(COOH)_n changed to surface inactive $\text{R-(COO}^-)_n$ with the acid-base reaction.[22] Thus, the driving force can be obtained by the development of a surface active molecular layer from solid R-(COOH)_n. In contrast, R-(COOH)_n is dissolved as $\text{R-(COO}^-)_n$ into the aqueous phase with HPO_4^{2-}, i.e., a driving force is not obtained.

The uniform motion for both camphanic acid and camphoric acid boats at the lower concentration is due to the successive development of a surface active layer as the driving force. The decrease in the velocity with an increase in the concentration of Na_2HPO_4 corresponds to a decrease in the driving force since the surface concentration of developed R-(COOH)_n decreases with an increase in the concentration of Na_2HPO_4. Intermittent oscillatory motion for a camphoric acid boat may be induced by the following mechanisms.[22] The camphoric acid molecules, which develop from the camphoric acid scraping, are ionized with phosphate ions, i.e., $\text{R(COOH)}_2 + 2\text{HPO}_4^{2-} \rightarrow \text{R(COO}^-)_2 + 2\text{H}_2\text{PO}_4^-$, around the aqueous surface (Step I). Therefore, the boat does not move. However, the concentration

of HPO_4^{2-} around the aqueous surface is decreased by the acid-base reaction, and a surface active camphoric acid layer can then easily develop on the aqueous surface (Step II). Therefore, the camphoric acid boat moves to another location with sufficient HPO_4^{2-}. Thus, intermittent oscillatory motion is generated by the repetition of Steps I and II. The increase in the resting time in intermittent motion with an increase in the concentration of HPO_4^{2-} (Fig.2b) suggests that the concentration of HPO_4^{2-} is sufficient in the resting state, and insufficient in the moving state. However, the above mechanism cannot explain why the camphanic acid boat does not show the oscillatory motion under the same experimental conditions as the camphoric acid boat.

4.2. Numerical simulation of the mode-change in the self-motion depending on the reaction order

To mathematically appreciate the motion of a camphor-derivative boat as an acid depending on the concentration of phosphate ions as a base, we introduce a mathematical model for an organic acid boat with an acid-base reaction in a linear cell. First, we assume that the organic acid disk is a material particle because of its sufficiently small volume, and approximate the organic acid boat as two rigid material particles:

$$\left(x_1(t), x_2(t)\right) = \left(x_c(t) + l, x_c(t) - l\right) \tag{2}$$

where $x_1(t)$, $x_2(t)$, and $x_c(t)$ denote the front of the plastic boat without organic acid, the rear of the plastic boat with organic acid, and the center, respectively. The length of the plastic boat is $2l$. The motion of the organic acid boat may be expressed by the following Newtonian equation:[22, 25, 28]

$$\rho \ddot{x}_c(t) = \frac{1}{2}\sum_{i=1}^{2} \frac{\partial}{\partial x}\gamma\left(u\left(t, x_i(t)\right)\right) - \mu \dot{x}_c(t), \tag{3}$$

where γ (N m^{-1}) is the surface tension at the air/water interface, $u(t, x)$ (mol m^{-2}) is the surface concentration of the surface active molecular layer developed from the solid disk, ρ (kg m^{-2}) is the surface density of the organic acid boat, and μ(kg m^{-2} s^{-1}) is a constant for the surface viscosity. Based on the general relationship between surface tension and the concentration of a surfactant,[22, 29] the surface tension may be expressed as a function of $u(t, x)$, as follows:

$$\gamma(u) = \frac{\gamma_0}{1 + a u^p} + \gamma_1 \tag{4}$$

where $\gamma_0 + \gamma_1$ (N m^{-1}) is the surface tension of water and γ_1 (N m^{-1}) is the minimum surface tension of water depending on the concentration of the surface active molecular layer.

We next consider a model for the following acid-base reaction:

$$m(\mathrm{H}_n\mathrm{A}) + n\mathrm{B} \xrightarrow{k_r} m\mathrm{A}^{n-} + n(\mathrm{B}^{m+}\text{-}\mathrm{H}_m), \tag{5}$$

where HA and B are acid and base. HA is ionized as A^- with B around the air/water interface.[22] Therefore, we can obtain the following reaction diffusion systems:

$$\begin{cases} \dfrac{\partial u}{\partial t} = D_u \dfrac{\partial^2 u}{\partial x^2} - k_d u - m k_r u^m v^n + F(x, x_2(t); r_0), \\ \dfrac{\partial v}{\partial t} = D_v \dfrac{\partial^2 v}{\partial x^2} - n k_r u^m v^n, \end{cases} \quad t>0,\ x\in(0,L), \tag{6}$$

where u (mol m^{-2}) is the surface concentration of HA at the air-water interface, v (mol m^{-3}) is the concentration of B near the air-water interface, D_u (m^2 s^{-1}) is the diffusion coefficient of the molecular layer of HA diffused to the air-water interface, D_v (m^2 s^{-1}) is the diffusion coefficient of B, k_d (s^{-1}) and k_r ($m^{2m+3n-2}$ mol^{1-m-n} s^{-1}) are the rate constants of dissolution and reaction, respectively, r_0 (m) is the radius of the disk, and L (m) is the length of the water bath. The function F (mol m^{-2} s^{-1}) reflects the development of a molecular layer of HA from the disk to the air/water interface. Although we approximate the disk as a material point in eq.3, we introduce a radius of the disk to consider the dependence on the size of the disk. Therefore, function F is defined as follows:

$$F(x, x_2(t); r_0) = \begin{cases} k_1 S_0, & |x - x_2(t)| \le r_0, \\ 0, & |x - x_2(t)| > r_0, \end{cases} \tag{7}$$

where S_0 is the constant amount to be supplied by the organic acid disk and k_1 is the rate of diffusion of the surface active organic acid layer from the solid disk. We assume that the decrease in the mass of the organic acid disk by diffusion of the organic acid layer is negligible, i.e., the mass of the disk is constant.

As a boundary condition, we take the following non-flux conditions:

$$\frac{\partial}{\partial x} u(t,0) = \frac{\partial}{\partial x} u(t,L) = 0, \quad \frac{\partial}{\partial x} v(t,0) = \frac{\partial}{\partial x} v(t,L) = 0. \tag{8}$$

To investigate the dependence on the concentration of B, we use the following initial conditions:

$$\begin{cases} u(0,x) \equiv 0, \quad v(0,x) \equiv v_0, \\ x_c(0) = x_{\mathrm{A}}, \quad \dot{x}_{\mathrm{c}}(0) = 0. \end{cases} \tag{9}$$

where v_0 is the initial concentration of B.

Finally, we require that $u(t,\cdot)$ is a continuously differentiable function on (0, L).

We now turn to the normalization of eqs.2-9. Let us introduce the following dimensionless parameters and variables:

$\tau = k_1 t,\ y = \sqrt{k_1 / D_u}\, x,\ y_k = \sqrt{k_1 / D_u}\, x_k \quad (k = 1, 2, c \text{ or } A),$

$U = u/S_0, V = v/v_0, D = D_v/D_u, \hat{\mu} = \mu / \rho k_1,\ \hat{l} = \sqrt{k_1 / D_u}\, l, \Gamma_0 = \gamma_0 /(D_u \rho k_1), \Gamma_1 = \gamma_1 /(D_u \rho k_1),$

$K_1 = k_d / k_1, K_2 = m S_0^{m-1} v_0^n k_r / k_1, K_3 = n S_0^m v_0^{n-1} k_r / k_1, R_0 = \sqrt{k_1 / D_u}\, r_0$, and $A = a S_0^p$.

If we rewrite τ, y, $y_k (k = 1, 2, c \text{ or } A)$, $\hat{\mu}$, $\hat{l}$ and $L_y = \sqrt{k_1 / D_u}\, L$ as $t, x, x_k (k = 1, 2, c \text{ or } A)$, μ, l, and L, respectively, we derive the following dimensionless model equations:

$$\begin{cases} \ddot{x}_{\mathrm{c}}(t) = \dfrac{1}{2} \displaystyle\sum_{\mathrm{i}=1}^{2} \frac{\partial}{\partial x} \Gamma\left(U\left(t, x_{\mathrm{i}}(t)\right)\right) - \mu \dot{x}_{\mathrm{c}}(t), \quad \mathrm{t} > 0, \\ \dfrac{\partial U}{\partial t} = \dfrac{\partial^2 U}{\partial x^2} - K_1 U - K_2 U^m V^n + F\left(x, x_2(t); R_0\right), \\ \qquad\qquad\qquad\qquad\qquad\qquad t > 0, x \in (0, L), \\ \dfrac{\partial V}{\partial t} = D \dfrac{\partial^2 V}{\partial x^2} - K_3 U^m V^n \end{cases} \tag{10}$$

with initial conditions

$$\begin{cases} U(0,x) \equiv 0, \quad V(0,x) \equiv 1 \\ x_c(0) = x_{\mathrm{A}}, \quad \dot{x}_{\mathrm{c}}(0) = 0, \end{cases} \tag{11}$$

and boundary conditions

$$\frac{\partial}{\partial x}U(t,0)=\frac{\partial}{\partial x}U(t,L)=0,\ \frac{\partial}{\partial x}V(t,0)=\frac{\partial}{\partial x}V(t,L)=0, \tag{12}$$

where $\Gamma(U)$ and $F(x, x_2; R_0)$ are expressed as

$$\Gamma(U)=\frac{\Gamma_0}{1+AU^p}+\Gamma_1 \tag{13}$$

and

$$F(x, x_2; R_0)=\begin{cases}1, & |x-x_2|\le R_0,\\ 0, & |x-x_2|>R_0.\end{cases} \tag{14}$$

We can perform our numerical simulation based on these dimensionless eqs. 10-14. Here, we change the parameter v_0 for comparison with the actual experiments. We assume that D is very small because the surface diffusion of the organic acid layer is significantly greater than the diffusion of base ion in the bulk phase.

Figures 3-5 show the numerical results for the motion of an organic acid boat depending on v_0 based on eqs.10-14 in the case of m =1 and n = 2. When v_0 is smaller than v_c, the boat moves at a constant velocity that decreases depending on v_0. When v_0 is larger than v_c, uniform motion changes to oscillatory motion, as shown in Fig. 3, and the period of oscillation increases depending on v_0, as shown in Fig. 5. These results suggest that the boat changes from uniform motion to oscillatory motion by Hopf bifurcation when v_0 increases.

In the case of m =1 and n=1, the velocity of the uniform motion of the boat monotonically decreases depending on v_0 without a change to oscillatory motion (data not shown). Finally, we numerically confirmed the mode-change from uniform motion to oscillatory motion depended on the reaction order m and n. Figure 6 shows the phase diagram for the mode of motion. If $m < n$, oscillatory motion appears, but if $m \geq n$, oscillatory motion does not appear. These results suggest that the present system includes Hopf bifurcation depending on m and n.

By using eqs. 10 and 13, we can explain why the change in the mode of motion is determined by the reaction order. If v_0 is very large in the case of m=1 and n>>1, the decreasing term, $-K_2U^mV^n$ is significantly larger than the increasing term, F, since K_2>>1. Therefore, $\frac{\partial \Gamma}{\partial x}(U) = 0$ in eqs. 10 and 13 because U cannot increase. As a result, the boat does not move (State I). However, $-K_2U^mV^n$ becomes less than 1 as V gradually decreases from 1 to 0 due to $-K_3U^mV^n$ in eq.10. Hence, U increases due to F, i.e., the organic acid layer can accumulate at the water surface. Accordingly, $\frac{\partial \Gamma}{\partial x}(U) \neq 0$ is obtained and therefore the organic acid boat moves to another point with V≡1 (State II). Thus, intermittent oscillatory motion occurs by the repetition of States I and II. On the other hand, the decreasing term, $-K_2U^mV^n$, is significantly small in the case of m>>1, n=1, and U < 1, even if K_2>>1 and V=1. Hence, U increases due to F. Therefore, the boat can exhibit uniform motion because of $\frac{\partial \Gamma}{\partial x}(U) \neq 0$. Thus, the model equations qualitatively reflect the experimental results of the camphoric acid-base reaction.

5. Conclusion

In this paper, the mode-bifurcation of self-motion was determined by the reaction

order for two substances (U, V) according to a numerical calculation. Numerical results were also determined for camphoric acid and camphanic acid boats depending on the concentration of Na_2HPO_4 in the water phase. To confirm the validity of the model equation, we should also consider other organic acids and base. In addition, we should consider the effect of the pK_a of the organic acids on the mode-bifurcation. Since pK_{a1} (= 4.57) for camphoric acid is close to pK_{a2} (= 5.10), the reaction order is approximated as m=1 and n=2. If pK_{a1} was significantly different from pK_{a2}, the reaction order would be m=1 and n=1 because the reaction would proceed successively rather than simultaneously. In fact, only uniform motion was observed when we examined benzene-1,3,5-tricarboxylic acid, which has pK_{a1}, pK_{a2}, and pK_{a3} values of 2.10, 4.10, and 5.18, respectively. The present study suggests that we may be able to create various manners of self-motion that depend on the kinetics of the chemical reaction and the chemical structure, such as pK_a.

Acknowledgments

We thank Prof. Hiroyuki Kitahata (Chiba University, Japan) and Prof. Shunsuke Izumi (Hiroshima University, Japan) for their helpful suggestions regarding the autonomous system. The present study was supported by Grants-in-Aid for Scientific Research (No. 20550124 to S.N and No. 18684002 to M.N) and by a grant from the Asahi Glass Foundation to S. N.

References

1 A. Mikhailov and D. Meinköhn, *Self-motion in Physico-Chemical Systems Far From Thermal Equilibrium*, Springer Berlin, Heidelberg, 1997, Vol. 484.

2 R. Yoshida, T. Sakai, S. Ito and T. Yamaguchi, *J. Am. Chem. Soc.*, 2002, **124**, 8095-8098.

3 É. Lorenceau and D. Quéré, *J. Fluid Mech.*, 2004, **510**, 29–45.

4 T. Yamaguchi and T. Shinbo, *Chem. Lett.*, 1989, 935-938.

5 K. Ichimura, S.-K. Oh and M. Nakagawa, *Science*, 2000, **288**, 1624–1626.

6 M. K. Chaudhury and G. M. Whitsides, *Science*, 1992, **256**, 1539-1541.

7 F. Brochard, *Langmuir*, 1989, **5**, 432-438.

8 T. Ichino, T. Asahi, H. Kitahata, N. Magome, K. Agladze, and K. Yoshikawa, *J. Phys. Chem. C*, 2008, **112**, 3032-3035.

9 Yu. Yu. Stoilov, *Langmuir*, 1998, **14**, 5685-5690.

10 C. Bain, G. Burnett-Hall and R. Montgomerie, *Nature*, 1994, **372**, 414-415.

11 F. Domingues dos Santos and T. Ondarçuhu, *Phys. Rev. Lett.*, 1995, **75**, 2972-2975.

12 S. Nakata, H. Komoto, K. Hayashi and M. Menzinger, *J. Phys. Chem. B*, 2000, **104**, 3589-3593.

13 W. F. Paxton, S. Sundarajan, T. E. Mallouk and A. Sen, *Angew. Chem. Int. Ed.*, 2006, **45**, 5420-5429.

14 Y.Sumino, N. Magome, T. Hamada and K. Yoshikawa, *Phys. Rev. Lett.* 2005, **94**, 068301-1–068301-4.

15 O. Schulz and M. Markus, *J. Phys. Chem. B*, 2007, **111**, 8175-8178.

16 P. G. Gennes, *Phys. A*, 1998, **249**, 196-205.

17 F. Jülicher, A. Ajdari and J. Prost, *Rev. Modern Phys.*, 1997, **69**, 1269-1281.

18 R. D. Astumian and M. Bier, *Phys. Rev. Lett.*, 1994, **72**, 1766-1769.

19 K. Sekimoto, *Prog. Theor. Phys.*, 1998, **130**, 17-27.

20 L. Rayleigh, *Proc. R. Soc. Lond.*, 1890, **47**, 364-367.

21 S. Nakata, Y. Iguchi, S. Ose, M. Kuboyama, T. Ishii and K. Yoshikawa, *Langmuir*, 1997, **13**, 4454-4458.

22 Y. Hayashima, M. Nagayama, Y. Doi, S. Nakata, M. Kimura and M. Iida, *Phys. Chem. Chem. Phys.*, 2002, **4**, 1386-1392.

23 S. Nakata, J. Kirisaka, Y. Arima and T. Ishii, *J. Phys. Chem. B*, 2006, **110**, 21131-21134.

24 S. Nakata and Y. Arima, *Coll. Surf. A*, 2008, **324**, 222–227.

25 Y. Hayashima, M. Nagayama and S. Nakata, *J. Phys. Chem. B*, 2001, **105**, 5353-5357.

26 M. I. Kohira, Y. Hayashima, M. Nagayama and S. Nakata, *Langmuir*, 2001, **17**, 7124-7129.

27 S. Nakata, Y. Doi and H. Kitahata, *J. Coll. Inter. Sci.*, 2004, **279**, 503-508.

28 M. Nagayama, S. Nakata, Y. Doi and Y. Hayashima, *Phys. D*, 2004, **194**, 151-165.

29 I. Langmuir, *J. Am. Chem. Soc.*, 1917, **39**, 1848-1906.

Figure captions

Figure 1. (a) Phase diagram of the mode of motion of camphanic acid (top) and camphoric acid (bottom) boats depending on the concentration of Na_2HPO_4 in the aqueous phase, and (b) time variation of the velocity of camphanic acid (top) and camphoric acid (bottom) boats with different concentrations of Na_2HPO_4 (0.02 M (1 and 3) and 0.08 M (2 and 4)). **U** and **O** denote uniform motion and intermittent oscillatory motion, respectively. (1) – (4) in (a) correspond to those in (b).

Figure 2. (a) Velocity of uniform motion and (b) period of intermittent motion of a camphoric acid boat depending on the concentration of Na_2HPO_4 in the aqueous phase.

Figure 3. Numerical results for the relation between the velocity of $x_c(t)$ and the parameter v_0, where μ=0.15, l=1.0, R_0=0.8, D=10^{-4}, k_d=0.5, k_r=2.0, k_1=1.0, m = 1, n = 2, S_0=1.0, A = 1.0, n_u = 2.0, Γ_0=1.0, Γ_1=0.5, x_A=4.0 and L = 40.0.

Figure 4. Numerical results on the time variation of the velocity of $x_c(t)$ at (a) v_0=5 (or K_2 = 50 and K_3 = 20), (b) v_0=20 (or K_2 = 800 and K_3 = 80), and (c) v_0=100 (or K_2 = 20000 and K_3 = 400). The parameters are the same as those in Fig. 3.

Figure 5. Period of oscillatory motion depending on the parameter v_0, where the parameters are the same as those in Fig. 3.

Figure 6. Numerical results on the phase diagram of the mode of motion depending on the reaction order, m versus n, where the parameters are the same as those in Fig. 3, except that v_0

= 20: U and O show uniform and oscillatory motion, respectively.

Figure 1

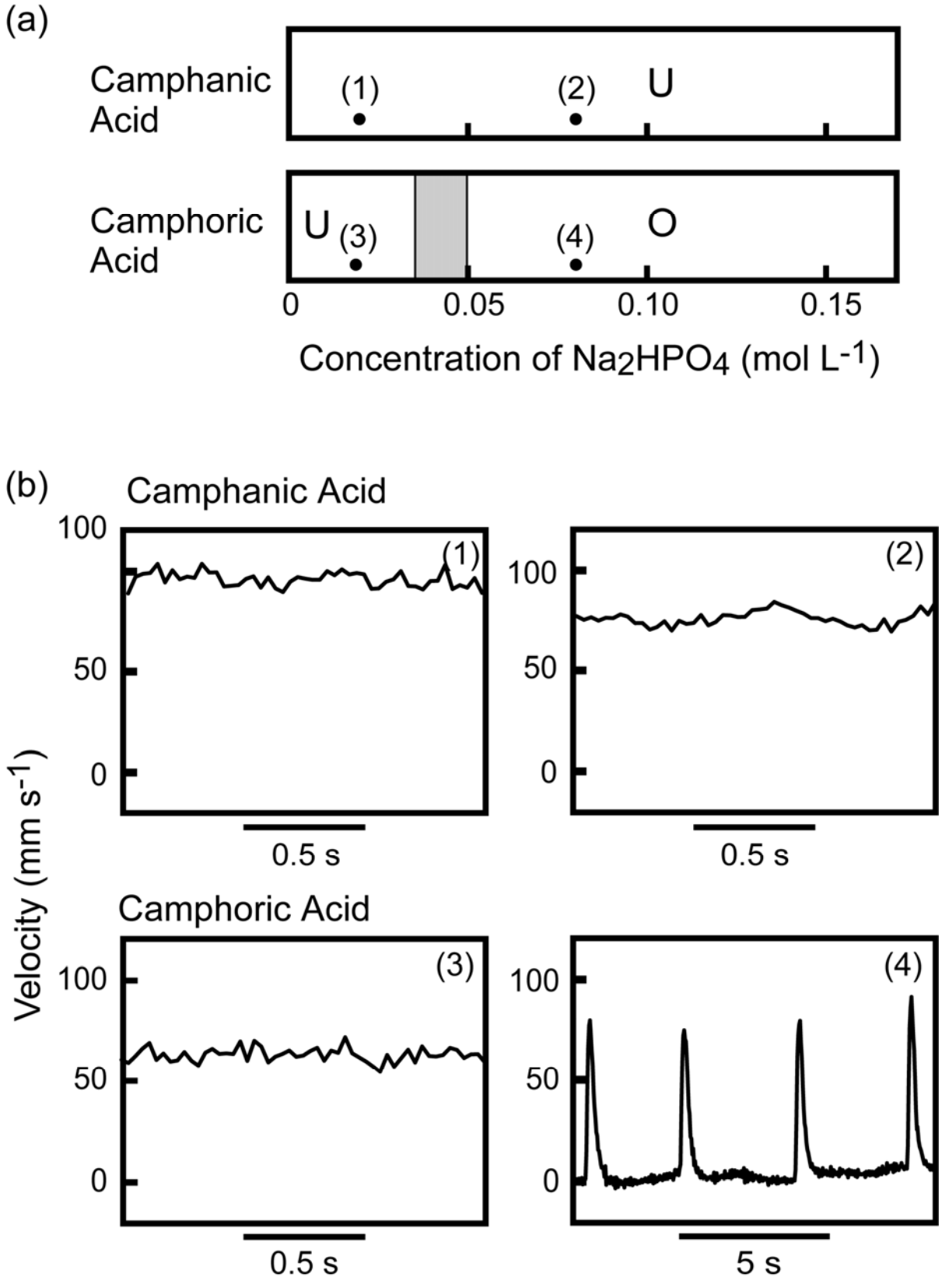
(a)
Camphanic Acid
(1)
(2)
U
Camphoric Acid
U
(3)
(4)
O
0
0.05
0.10
0.15
Concentration of Na2HPO4 (mol L-1)
(b)
Camphanic Acid
100
50
0
(1)
0.5 s
(2)
0.5 s
Velocity (mm s-1)
Camphoric Acid
(3)
0.5 s
(4)
5 s

Figure 2

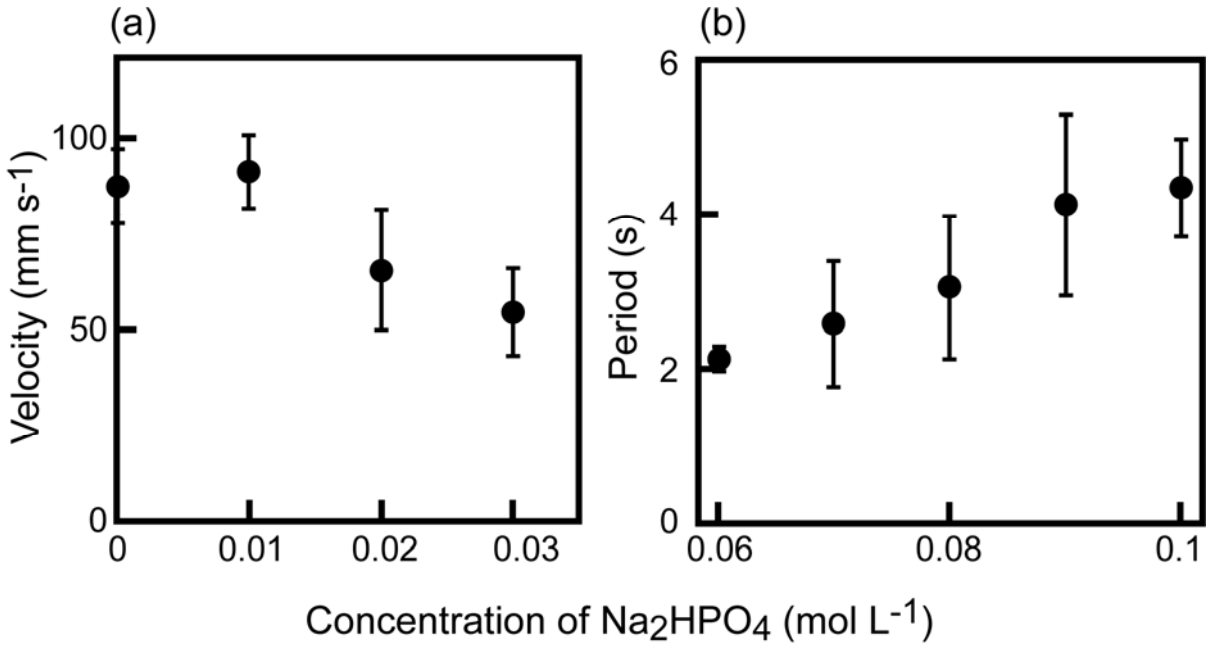
(a)
(b)
Velocity (mm s-1)
Period (s)
100
50
0
6
4
2
0
0
0.01
0.02
0.03
0.06
0.08
0.1
Concentration of Na2HPO4 (mol L-1)

Figure 3

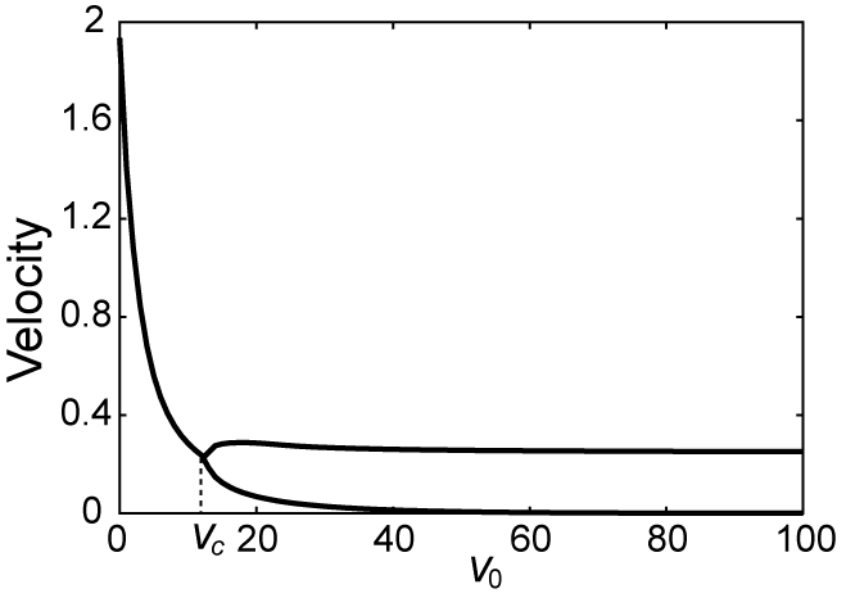

Figure 4

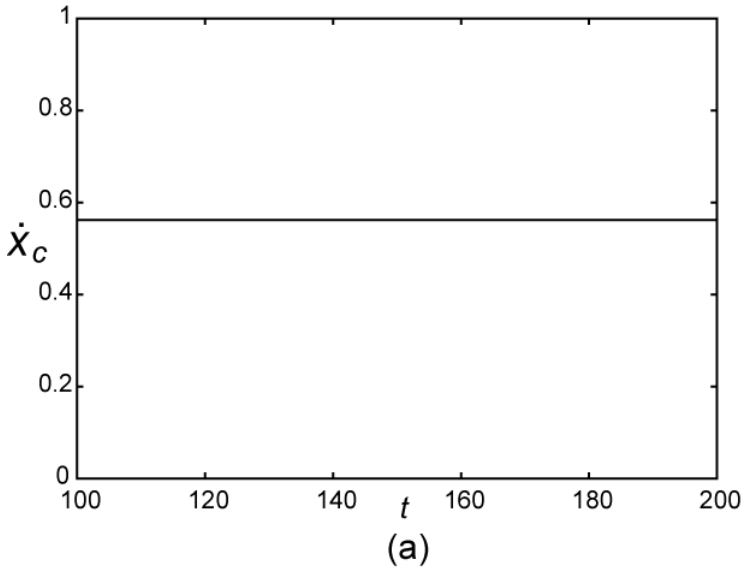
1
0.8
0.6
$\dot{x}_c$
0.4
0.2
0
100
120
140
160
180
200
t

(a)

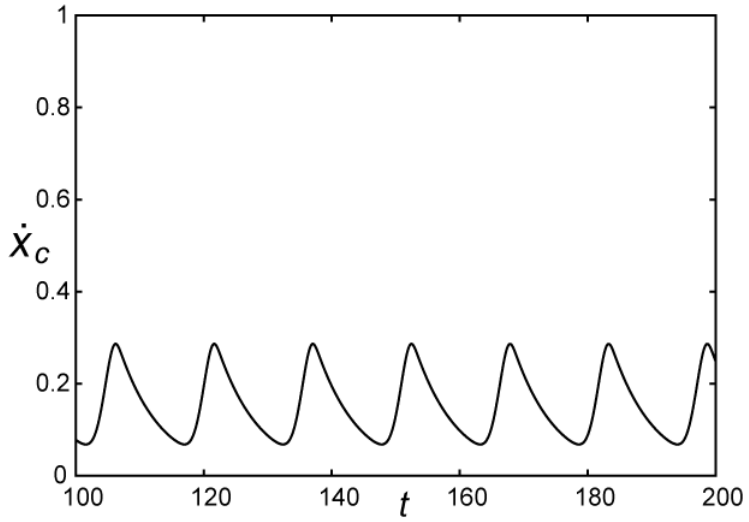
1
0.8
0.6
$\dot{x}_c$
0.4
0.2
0
100
120
140
160
180
200
t

(b)

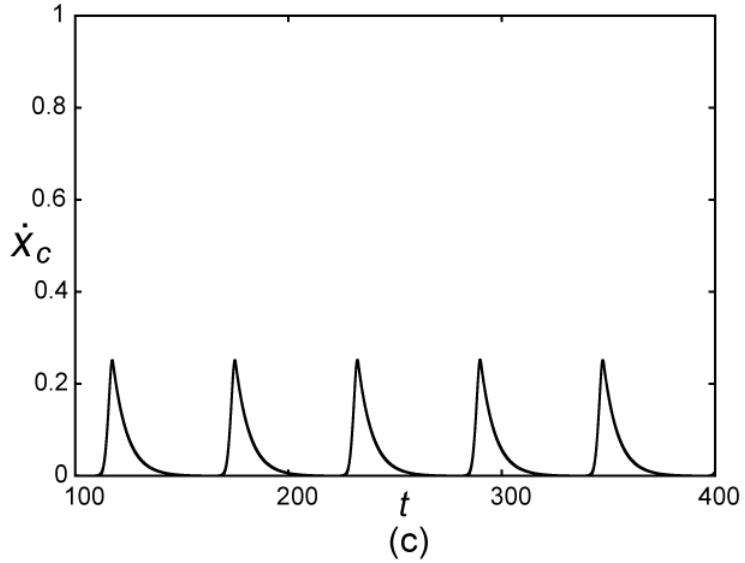
1
0.8
0.6
$\dot{x}_c$
0.4
0.2
0
100
200
300
400
t

(c)

Figure 5

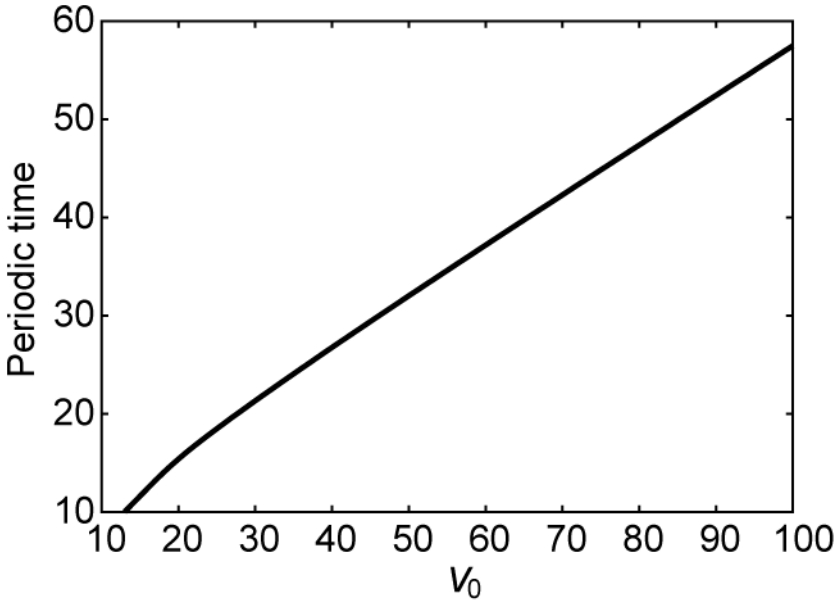

Figure 6